Saudi Journal of Biological Sciences (2017) 24, 1547–1554

King Saud University

Saudi Journal of Biological Sciences

www.ksu.edu.sa
www.sciencedirect.com

ORIGINAL ARTICLE

Effects of hematite and ferrihydrite nanoparticles on germination and growth of maize seedlings

Nicolaza Pariona [a,b], Arturo I. Martinez [a,*], H.M. Hdz-García [c], Luis A. Cruz [b], Adolfo Hernandez-Valdes [a]

[a] Center for Research and Advanced Studies of the National Polytechnic Institute, Cinvestav-Saltillo, 25900 Ramos Arizpe, Coahuila, Mexico
[b] Red de Estudios Moleculares Avanzados, Instituto de Ecología A.C., Carretera Antigua a Coatepec 351, El Haya, 91070 Xalapa, Veracruz, Mexico
[c] Corporación Mexicana de Investigación en Materiales S.A. de C.V., Ciencia Y Tecnología 790, Fracc. Saltillo 400, 25290 Saltillo, Coahuila, Mexico

Received 7 January 2016; revised 20 April 2016; accepted 12 June 2016
Available online 17 June 2016

KEYWORDS

Nanoparticles uptake;
Iron oxides;
Food crops;
Phytotoxic effects;
Zea mays;
Translocation

Abstract Engineered iron oxide nanoparticles (IO-NPs) have been used extensively for environmental remediation. It may cause the release IO-NPs to the environment affecting the functions of ecosystems. Plants are an important component of ecosystems and can be used for the evaluation of overall fate, transport and exposure pathways of IO-NPs in the environment. In this work, the effects of engineered ferrihydrite and hematite NPs on the germination and growth of maize are studied. The germination and growth of maize were done with treatments at different concentrations of hematite and ferrihydrite NPs, namely 1, 2, 4, and 6 g/L. Biological indicators of toxicity or stress in maize seedlings were not observed in treatments with engineered hematite and ferrihydrite NPs. In contrast, the NPs treatments increased the growth of maize and the chlorophyll content, except for hematite NPs at 6 g/L, where non-significant effects were found. The translocation of engineered ferrihydrite and hematite NPs in maize stems was demonstrated using confocal laser scanning microscopy.

1. Introduction

Currently, nanoscience and nanotechnology have attracted great attention; it is because nanomaterials exhibit fascinating properties arising from their small scale. Particularly, iron oxide (IO) nanoparticles (NPs) are a focus of interest because of their potential applications in environmental remediation and biomedicine (Di Bona et al., 2015, 2014; Faraji et al., 2010; Indira and Lakshmi, 2010). Specific environmental applications of IO-NPs are arsenic removal technologies

* Corresponding author.
E-mail address: mtz.art@gmail.com (A.I. Martinez).
Peer review under responsibility of King Saud University.

Production and hosting by Elsevier

http://dx.doi.org/10.1016/j.sjbs.2016.06.004
1319-562X

(Giménez et al., 2007; Richmond et al., 2004), and Fenton-like catalysts for the degradation of aqueous organic solutes (Bokare and Choi, 2014; Xue et al., 2009). Iron is an essential element for living organism and is the fourth most common element in the Earth's crust. However, due to the release of engineered IO-NPs to the environment, they may affect the functions of ecosystems.

Plants are an important component of ecosystems and can be used for the evaluation of overall fate, transport and exposure pathways of NPs in the environment (Bombin et al., 2015; Zhu et al., 2008). A few works have reported the effects of IO-NPs on the germination and growth of plants. For example, it has been reported that daily additions of Fe_3O_4-NPs in the presence of static magnetic fields, increased the growth of *Zea mayz* and the levels of chlorophyll (Răcuciu and Creangă, 2007). Increased chlorophyll levels have also been reported in soybean seedlings treated with 9 nm Fe_3O_4-NPs applied in a concentration based on iron concentration needed for plant growth; no trace of toxicity but translocation into soy bean stems was reported (Mahmoudi, 2013). Furthermore, it has been found that aqueous suspensions of Fe_3O_4-NPs can be translocated throughout pumpkin plant tissues and accumulated into the roots and leaves (Zhu et al., 2008).

Additionally, the biological effects of 9 and 18 nm γ-Fe_2O_3-NPs towards watermelon seedlings have been evaluated; it was found that the treatments with NPs increased different biological indicators such as seed germination, seedling growth, and larger activities of catalase, peroxidase (POD) and superoxide dismutase (SOD) were reported (Li et al., 2013). Otherwise, the phytotoxicity of Fe_2O_3-NPs of 20–40 nm in concentrations from 0 to 5 g/L was evaluated for lettuce, radish and cucumber seeds, where no significant phytotoxic effects were reported (Wu et al., 2012). In addition, the phytotoxicity of 6 nm γ-Fe_2O_3-NPs in concentrations from 0 to 2 g/L on rice plants has been reported; a significantly higher root elongation in treated plants with respect to the control was found (Alidoust and Isoda, 2014). It was concluded that the phytotoxicity of γ-Fe_2O_3-NPs is small and even lower than the phytotoxicity of bulk γ-Fe_2O_3 (Alidoust and Isoda, 2014). In a very recent work, the response of transgenic and conventional rice to γ-Fe_2O_3-NPs was studied (Gui et al., 2015). It was found that upon exposure to γ-Fe_2O_3-NPs, the activities of SOD and POD of transgenic rice were notably higher than the control; otherwise, in non-transgenic rice, their activities varied slightly but not significantly among treatments (Gui et al., 2015).

It has been shown that IO-NPs (Fe_3O_4 and γ-Fe_2O_3) could affect positively different plant growth performance indicators such as root and stem elongation, increased chlorophyll levels, and larger activities of catalase, POD and SOD. Thus the use of IO-NPs opens a wide range of possibilities in plant research and agronomy (González-Melendi et al., 2008). However, to the best of our knowledge, any work has been reported for the evaluation of the effects of other IO-NPs on the growth of plants. Hematite (α-Fe_2O_3) and ferrihydrite ($5Fe_2O_3{\cdot}9H_2O$) NPs were selected here because these engineered NPs are widely applied in environmental remediation of water and soils. It is important to mention that hematite is the most stable iron oxide polymorph, and ferrihydrite is a metastable poorly crystallized phase which occurs in natural media in form of NPs (Jambor and Dutrizac, 1998; Schwertmann and Cornell, 2000). In addition, despite metastability of ferrihydrite, in natural environments, the presence of soluble silicate species and organic matter inhibits its transformation to more crystalline IOs. Naturally occurring ferrihydrite NPs have been detected in a great variety of agriculturally productive terrains such as loess, peat bog, and paddy fields (Jambor and Dutrizac, 1998).

Given the importance of both hematite and ferrihydrite NPs, it is imperative to study their effects on the growth of different plants. For this study, maize was selected because it constitutes a staple food in many regions of the world, especially in Mexico, where maize is a central ingredient in Mexican food. The aim of this work is to study the effects of engineered hematite and ferrihydrite NPs on different biological indicators, their uptake, and translocation on maize seedlings.

2. Experimental details

2.1. Synthesis and characterization of IO-NPs

All chemicals were of analytical grade and used as received without further purification. The 2-line ferrihydrite NPs were prepared following a slightly modified reported procedure Schwertmann and Cornell, 2000. Firstly, under constant stirring, 6 mL of 6.0 M NaOH was added to 100 mL of 0.3 M $FeCl_3$. In order to reach a pH of 8.0, some drops of 1.0 M NaOH were added to the reaction media. Once obtaining the ferrihydrite NPs, they were washed several times with deionized water and dried at room temperature (RT) for 48 h. For the preparation of the hematite NPs, the suspension of freshly prepared ferrihydrite NPs was stirred for 10 min. After that, 0.16 g of $FeSO_4{\cdot}7H_2O$ (atomic ratio of Fe(II)/Fe(III) = 0.02) was added, this decreased the pH to 6.5, then the reaction medium was carefully adjusted to pH 9.0 with 1.0 M NaOH. Subsequently, 5 mL of a pH buffer of 1 M $NaHCO_3$ was added. The reaction was stirred at 95 °C for 120 min; it yielded hematite NPs, which were washed by the same procedure described above and dried at RT for 48 h.

The structural properties of the synthesized powders were studied by X-ray diffraction (XRD) and transmission electron microscopy (TEM). For XRD, a Philips diffractometer X'Pert with the Cu(Kα) radiation in a 2-θ range of 20–80° was used. For the TEM analyses, samples were prepared by dispersing the NPs in ethanol; this dispersion was dropped onto 300 mesh holey lacey carbon grids and observed in a FEI Titan microscope operated at 300 kV.

2.2. Seed germination and early growth

Maize (*Z. Mays*) seeds were donated by the Antonio Narro Agrarian Autonomous University, Saltillo, Mexico. In order to evaluate the effects of IO-NPs on germination of maize, the seeds were washed with deionized water (DIW) and placed at 4 °C before experiments. Furthermore, the suspensions of IO-NPs were prepared by ultrasonicating different amounts of ferrihydrite and hematite in DIW for 30 min (Lin and Xing, 2007); it yielded suspensions of 1, 2, 4 and 6 g/L, which were used as treatments. After this, the seeds were submerged for 1 h in the suspensions of IO-NPs, and subsequently 10 seeds were placed on sterile paper in Petri dishes along with 10 mL of the respective suspension. For the control, only distilled water was added to the Petri dishes (U.S. Environmental

Protection Agency, 1996). The seeds were germinated in covered Petri dishes for 4 days in a growth chamber at 23 °C in a dark place. The seeds were considered as germinated when the radicle showed at least 2 mm in length (U.S. Environmental Protection Agency, 1996).

After germination, the maize seedlings were transferred onto sterile paper on new Petri dishes, and 20 mL of suspensions of IO-NPs at the concentrations mentioned above were added. In order to satisfy the nutrient requirements of the seedlings, along with the NPs, an adequate hydroponic nutrient solution for maize was used (Smith et al., 1983). For the control, only DIW and nutrient solution was added to the Petri dishes. The seedlings were grown for 12 days in a growth chamber at RT, 65% relative humidity, 16/8 light/dark photoperiod, and irrigated with DIW daily. For statistical purposes, each treatment was replicated three times.

After 12 days of growth, the chlorophyll content index (CCI) was measured on the second fully expanded leaf on the top of the main stem of each seedling using an Opti-Sciences CCM-200 chlorophyll meter. The CCI is based on absorbance measurements at 660 and 940 nm, which is proportional to the concentration of chlorophyll. CCI data were recorded at three positions along the length of the leaf and averaged as a single value. Subsequently, the seedlings were washed with DIW three times, and the length of roots, stems, and leaves were measured. In order to evaluate the dry biomass of roots, stems and leaves, they were dried in an incubator at 60 °C for 72 h (Siddiqui and Al-Whaibi, 2014; Wang et al., 2012).

2.3. Microscopic evidence of uptake of hematite and ferrihydrite NPs

3D microscopic techniques were employed for the observation of plant tissues treated with the IO-NPs and the control. For the observations, two stems were randomly selected from specimens treated with suspensions of hematite and ferrihydrite (6 g/L) and the control. The samples were treated according to previous literature (González-Melendi et al., 2008). Stems sections were perfectly immersed in the fixative, which consisted of 5 mL of formaldehyde, 5 mL of acetic acid, and 90 mL of 70/30 (v/v) ethanol/DIW. For paraffin embedding, the samples were dehydrated at RT using a graded ethanol series (50%, 60%, 70%, 85%, 96%, and twice at 100% (v/v) ethanol/DIW) with 30 min exposure at each step. Subsequently, the samples were treated in xylene/ethanol (3/1, 1/1, 1/3, and twice in pure xylene for 2 h in each treatment). After that, the samples were stored in xylene/paraffin at 30 °C for 24 h, after this step, more paraffin was added (saturation) at 55 °C. Finally, the xylene/paraffin mixture was decanted, and the samples were transferred to flat embedding molds. After 24 h, transversal and longitudinal cuts with a thickness of 15 μm were done in a microtome. Before microscope observations, the paraffin was removed from the tissues with xylene/alcohol (95%, 85%, 70%, 60%, and 50% v/v) washes for 10 min, and rehydrated with DIW for 1 h. Finally, the samples were dried at RT for 24 h and mounted in Canada balsam.

Sections were examined in a confocal laser-scanning microscope Leica TCS SP8, where the confocal setup is based on a DMI6000 inverted microscope. An excitation and emission spectral study was done with lasers of 405, 488, 528, and 635 nm. The auto-florescence of plant tissues was excited with the 488 nm laser and the emission was collected in the range of 509–557 nm, which represents the green color on the micrographs. The presence of hematite and ferrihydrite NPs was detected by reflection of the 635 nm laser and the reflected signal was collected in the range of 635–650 nm.

Moreover, the iron concentration was determined in maize leaves. For this, 1.0 g of the dry leaves was digested with 16 mL of 6/2 v/v HNO_3/H_2O_2 for 2 h at 120 °C (Marin et al., 2011). Then 10 mL of DIW was added. After cooling, 10 mL of DIW was added and mixed. The residue was filtered through filter paper and diluted to 50 mL with DIW. The iron concentrations were determined by the inductively coupled plasma/emission spectroscopy (ICP-MS-Thermo elemental IRIS-Intrepid II).

2.4. Statistical analysis

One-way analysis of variance (ANOVA) and Fisher LSD multiple range tests with a significance level of 95% ($p < 0.05$) were used to determinate statistical differences between treatments. All statistical analyzes were performed using the Statistica 8.0 software package.

3. Results and discussion

3.1. Characterization of NPs

Both ferrihydrite and hematite NPs were prepared by green synthesis methods, because instead of toxic organic solvents, water was utilized as an environmentally benign solvent. Fig. 1(a) shows the XRD pattern of the synthetized hematite NPs. The XRD pattern of the sample was indexed to the rhombohedral structure of hematite JCPDS card No. 89-598 (see vertical lines). The average crystallite size obtained by Rietveld refinement was of 100 nm. Fig. 1(b) shows the TEM

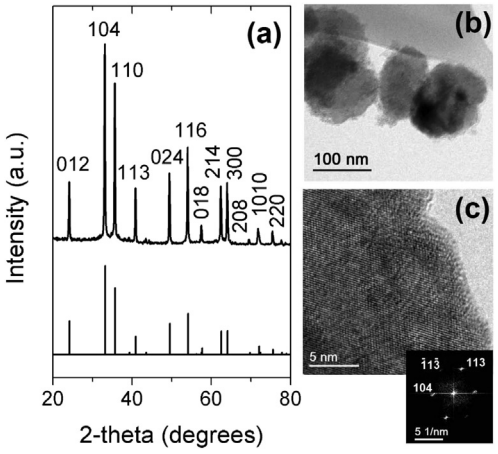

Figure 1 Structural characterization of the hematite NPs. (a) XRD pattern indexed to the rhombohedral structure of hematite JCPDS card No. 89-598 (vertical lines). (b) TEM micrograph of hematite NPs. (c) HR-TEM image of the lattice fringes of a hematite NP, the inset shows the FFT image showing the spot pattern indexed to the crystal planes of the hematite structure.

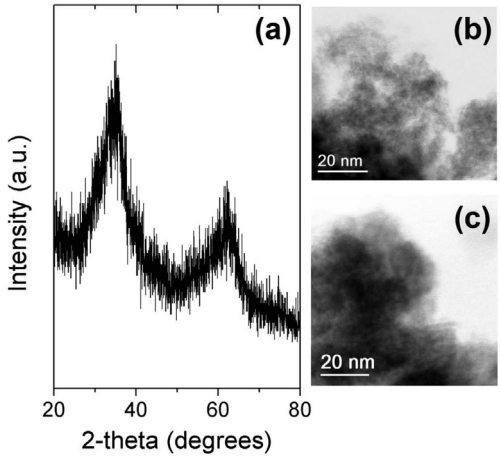

Figure 2 Structural characterization of the ferrihydrite NPs. (a) XRD pattern of the sample exhibiting a typical pattern of 2-line ferrihydrite. (b, c) TEM micrographs of clusters of ferrihydrite NPs.

images of the hematite NPs, it displays some particles of *ca.* 100 nm with an ovoid and rounded shape. Fig. 1(c) shows a HR-TEM image in the border of a hematite particle where the lattice fringes are clearly seen, the FFT image shown in the inset displays spot patterns corresponding to the (1 0 4), and (1 1 3) crystal planes of hematite. Fig. 2(a) shows the XRD pattern of the synthetized ferrihydrite NPs. It can be observed that ferrihydrite exhibits two wide peaks centered at *ca.* 35 and 62 2-θ degrees, similar XRD patterns have been reported for 2-line ferrihydrite (Liu et al., 2009; Schwertmann and Cornell, 2000). Fig. 2(b) and (c) shows the TEM images of the ferrihydrite NPs; they display clusters of strongly aggregated particles of *ca.* 3 nm.

3.2. Germination and seedling growth of maize

The effect of hematite and ferrihydrite on the germination of maize seeds is shown in Fig. 3(a). As seen in the figure, at the evaluated concentrations of both hematite and ferrihydrite, none of the treatments affected the seed germination % with respect to the control ($p \geqslant 0.11$). Nevertheless, it can be observed that the germination % increased slightly with the ferrihydrite NP treatments. In the literature, different impacts of IO-NPs on germination % have been reported, which depend on different factors such as the type of plant, the iron oxide polymorph, the size of the NPs, and the concentration of the NPs in each application. For example, it has been reported that the germination % of Chinese mung bean decreased by the application of maghemite NPs in a concentration of 10 mg/L (Hong-Xuan et al., 2011). On the other hand, using magnetite treatments in a concentration of 116 mg/L on cucumber and lettuce seeds, a decrease of germination % was reported (Barrena et al., 2009). Despite this, to the best of our knowledge, the mechanism of interaction between the IO-NPs and seeds during germination has not been elucidated.

The chlorophyll content index in seedlings treated with hematite, ferrihydrite, and the control is presented in Fig. 3 (b). For most of the treatments, the CCI is not strongly affected with respect to the control ($p \geqslant 0.057$); except for the 2 g/L ferrihydrite treatment which is 18% higher compared with the control ($p = 0.048$). Similar results have been reported in watermelon (Li et al., 2013) and Chinese mung bean (Hong-Xuan et al., 2011) treated with magnetite NPs of 9 and 18 nm, where the chlorophyll content compared to control was not significantly affected. Nevertheless, they found increments lower than 10% of chlorophyll content with respect to their controls. Additionally, in lettuce plants treated with core–shell Fe/Fe_3O_4 NPs in a 10 mg/L treatment, the chlorophyll content increased with respect to the control by 12% (Trujillo-Reyes et al., 2014).

Fig. 4 shows different parameters that indicate the growth of plants treated with the IO-NPs suspensions. Hematite at a concentration of 1, 2, and 4 g/L increased the root's length by 73%, 67%, and 63%, in relation to the control ($p \leqslant 0.0001$). Otherwise, for ferrihydrite at 1, 2, 4, and 6 g/L increased the root's length by 55%, 54%, 39%, and 29% in relation to the control ($p \leqslant 0.03$). Additionally, the length of both stems and leaves increased in most of the hematite and ferrihydrite treatments in relation to the control. However, despite root's length exhibiting a trend (higher concentrations of NPs promoted lower increases of roots length), no trends were observed in the stem and leaves length. The highest values of stems and leaves length were observed with treatments with ferrihydrite NPs at 4 g/L, which increased 30% and 35% in relation to the control ($p \leqslant 0.0005$), respectively (Fig. 4b and c).

Dry weight of roots, stems and leaves behave in a similar way to their corresponding lengths, see Fig. 4(d–f). The highest root mass was found in the hematite treatment (4 g/L) which increased 23% in relation to the control ($p = 0.06$). Otherwise, for both stems and leaves mass, the highest values were found in the ferrihydrite treatment (4 g/L), by 36%, and 83%, respectively, in relation to the control ($p \leqslant 0.03$). Furthermore, for the hematite treatment at 6 g/L reduced root mass by 18% in relation to the control ($p = 0.14$) was observed, which is the sole value that shows a reduction in relation to the control for all the treatments with IO-NPs.

Biological indicators of toxicity or stress in plants such as reduction of chlorophyll content, and inhibition of plant growth were not observed in this work with hematite and ferrihydrite NP treatments at very high concentrations. In contrast, the treatments applied here increased the growth of maize and the chlorophyll content. Similar results have been observed in previous works using magnetite and maghemite NPs (Alidoust and Isoda, 2014; Li et al., 2013).

3.3. Microscopic evidence of translocation of IO-NPs in maize stems

The possibility of entry and translocation of hematite and ferrihydrite NPs in maize stems was studied by 3D microscopic techniques. Fig. 5 shows transversal and longitudinal cuts of maize stems treated with hematite NPs, ferrihydrite NPs and the control. In the micrographs, the green color represents the autofluorescence of plants tissues, while the red color represents the aggregates of either hematite or ferrihydrite NPs.

Fig. 5(a and b) shows the transversal and longitudinal maize stem cuts of the control treatment, these micrographs show the tissue of maize stems in green, and the absence of red dots was confirmed in different cuts. In contrast, for maize

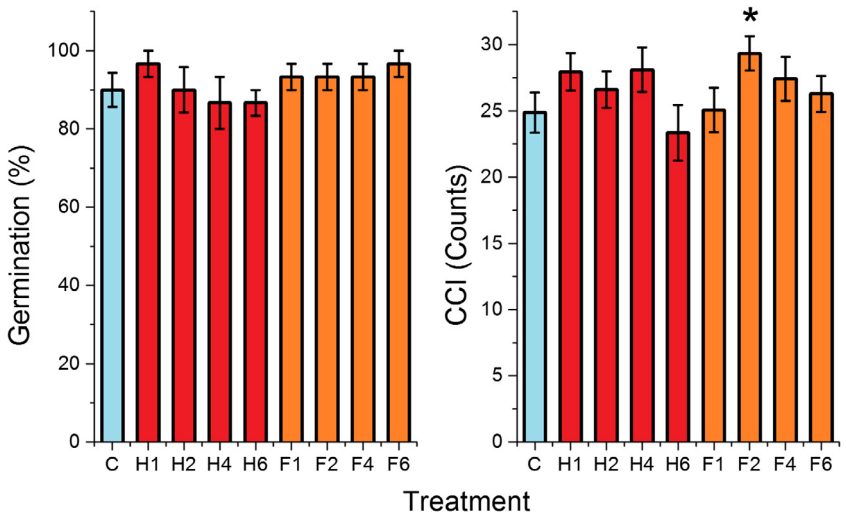

Figure 3 (a) Germination percentage of maize seeds treated with hematite (H), ferrihydrite (F), and the control (C). (b) Chlorophyll content index in seedlings treated with hematite (H), ferrihydrite (F), and the control (C). The numbers next to H and F indicate the concentration of the NPs in the treatment in g/L. *Stands for statistical differences with respect to the control ($p \leqslant 0.05$).

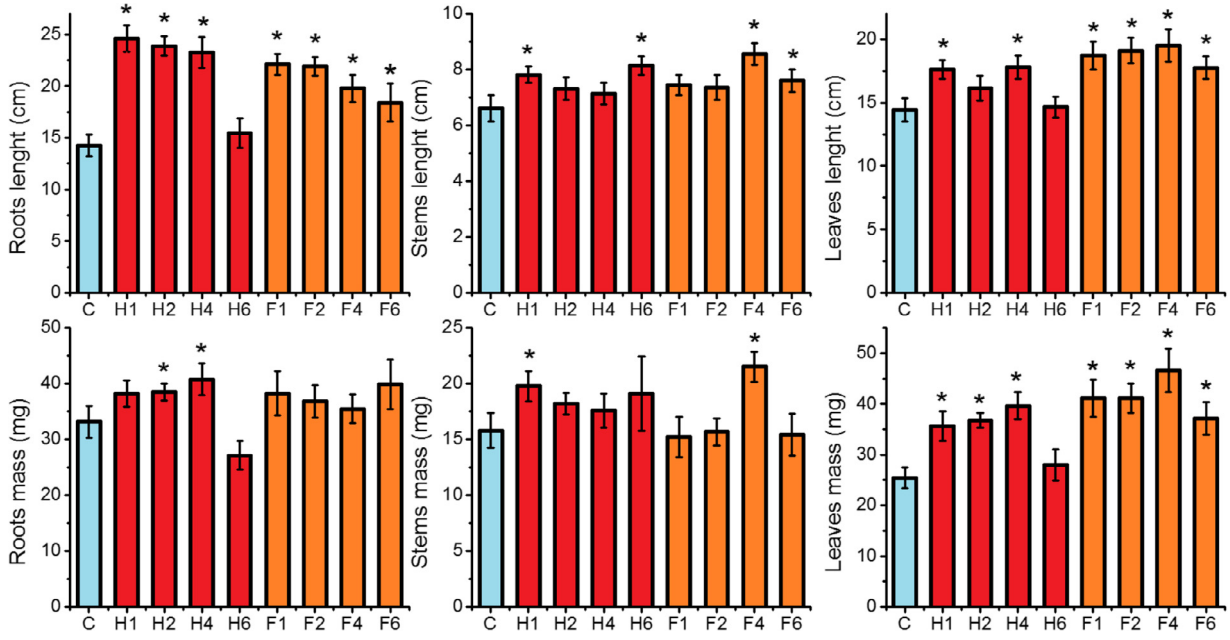

Figure 4 Length (a–c) and mass (d–f) of roots, stems and leaves of maize seedlings treated with hematite (H), ferrihydrite (F), and the control (C). The numbers next to H and F indicate the concentration of the NPs in the treatment in g/L. *Stands for statistical differences with respect to the control ($p \leqslant 0.05$).

seedlings treated with ferrihydrite and hematite NPs, the transversal and longitudinal stems cuts shown in Fig. 5(c–f), red particles of different sizes are observed inside the endodermis and vascular bundles. These red particles were assigned to clusters of either hematite or ferrihydrite NPs, the sizes of these agglomerates ranges from 0.6 to 2 μm. Thus, the micrographs shown in Fig. 5(c–f) reveal that the IO-NPs have been translocated into maize stems treated with hematite and ferrihydrite NPs.

The clusters of hematite and ferrihydrite NPs displayed in Fig. 5(c–f) are located in xylem and phloem vessels, and in cell walls of xylem vessels. Moreover, longitudinal sections displayed reveal that the IO-NPs are transported through both the apoplastic pathway to the endodermis and the symplastic pathway to the vascular system (Fig. 5d and f). Similar results have been reported for the uptake and translocation of ZnO NPs in maize seedlings (Zhao et al., 2012).

In addition to the microscopic evidence of translocation of IO-NPs in maize stems, the iron content in maize leaves was determined. Fig. 6 shows the iron concentrations of maize leaves treated with different concentrations of hematite NPs, ferrihydrite NPs and the control. In all the hematite and ferri-

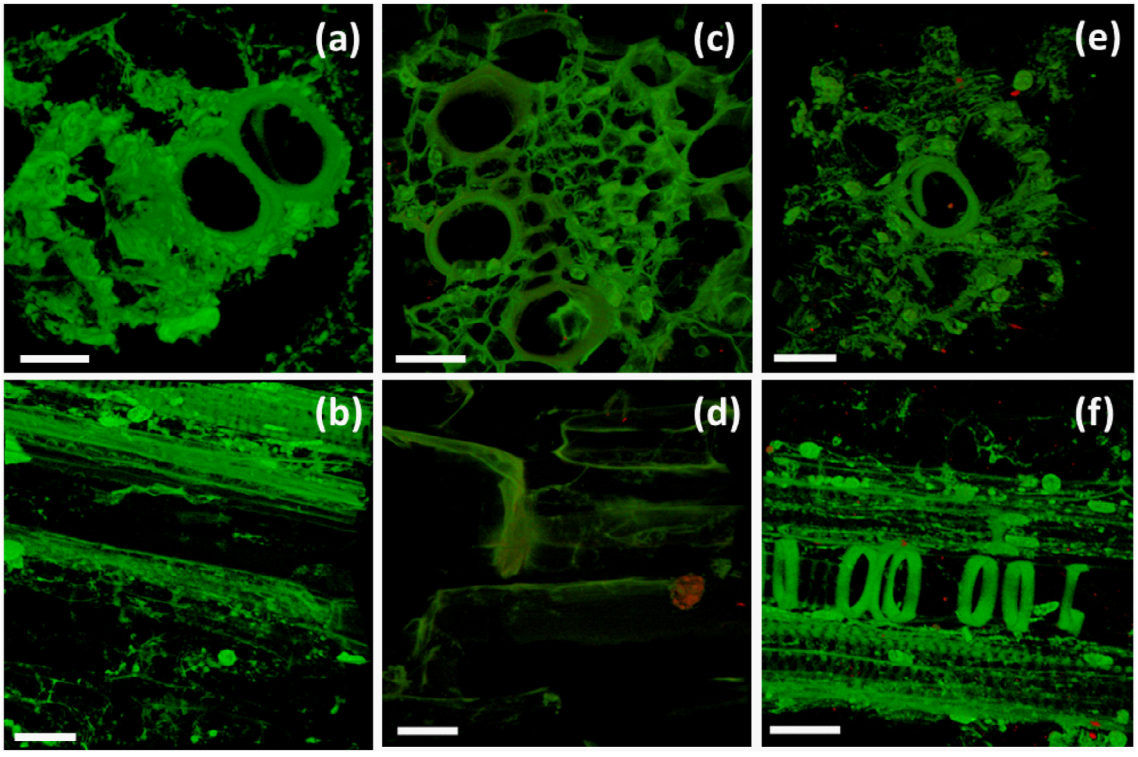

Figure 5 3D micrographs of transversal (on top) and longitudinal (on bottom) cuts of maize stems treated with the control (a, b), hematite NPs (c, d), and ferrihydrite NPs (e, f). The scale bars represent 30 μm.

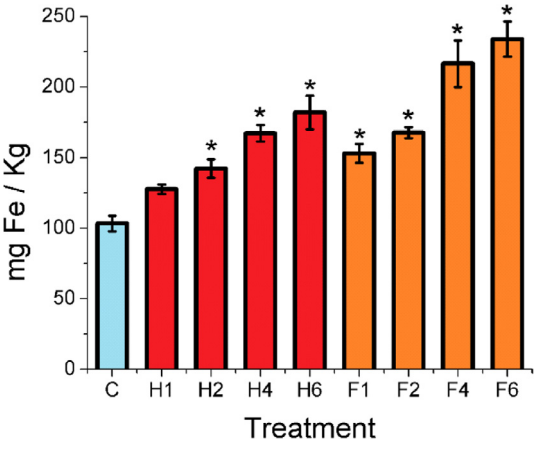

Figure 6 Effects of hematite (H) and ferrihydrite (F) NPs on iron uptake by maize seedlings. The numbers next to H and F indicate the concentration of the NPs in the treatment in g/L. *Stands for statistical differences with respect to the control ($p \leqslant 0.05$).

hydrite NP treatments showed increased concentrations of iron in leaves compared to the control. However, the ferrihydrite treatments exhibited higher concentrations than the hematite treatments at the same concentration. For example, the treatments with a concentration of 6 g/L of both hematite and ferrihydrite NPs increased the iron content in leaves by 76% and 127%, respectively, compared to the control. It means that the ferrihydrite NPs are taken by maize roots, travel through the stem and are accumulated in leaves in a major extend than hematite NPs. These results suggest that clusters of IO-NPs were absorbed by root tip cells, subsequently, the IO-NPs were internalized into cells walls, embedded by new cells, later, they enter into the vascular system, and are accumulated in maize leaves (Lv et al., 2015). This transportation system could be the way that IO-NPs aggregates take into the maize seedling.

Iron constitutes an essential element for the optimal growth of plants, as well as their biomass and fruit production (Briat et al., 2010). Iron plays an important role for the structure and/or function of the photosynthetic electron transfer chain (Briat et al., 2015). Additionally, the photosynthetic efficiency, the structure and function of the photosynthetic apparatus are heavily iron-dependent, directly or indirectly via the porphyrin biosynthesis pathway (Briat et al., 2015). It has been reported that iron deficiency leads to a decrease in the chlorophyll concentration, which affects the photosynthetic metabolism and the development of plants (Briat et al., 2010, 2007). In contrast, iron excess may cause oxidative stress (Briat et al., 2010). In this way, intracellular iron homeostasis is very important, where phytoferritin plays a crucial role. This protein storages iron into its nanocage in the form of iron minerals such as ferrihydrite of 5–10 nm in size (Schwertmann and Cornell, 2000). It is well known that phytoferritin is of great importance in seed germination. During this process, phytoferritin is degraded and releases iron, it promotes the generation of hydroxyl ions that destroys the protein layer of the seed (Lobreaux and Briat, 1991; Zhang et al., 2013).

It was shown that engineered hematite and ferrihydrite NPs were translocated into maize stems, and these NPs do not negatively affect both the development of maize seedlings and the

germination of maize seeds. It can be assumed that the IO-NPs translocated in the plants act as phytoferritin cores, where they are not completely dissolved and may work as iron suppliers. Thus, it is suggested that the iron supplied by the engineered IO-NPs influence the biosynthesis of chlorophyll and promotes better biomass yields. Given the role of iron in the germination and development of plants, and that a controlled addition of the engineered IO-NPs may improve the growth of plants. It can be concluded that the IO-NPs may act as iron source for plants and to be used as fertilizers.

4. Conclusions

Biological indicators of toxicity or stress in maize seedlings were not observed in treatments with engineered hematite and ferrihydrite NPs. In contrast, the NP treatments increased the growth of maize and the chlorophyll content. Similar results have been observed in previous works using other engineered IO-NPs such as magnetite and maghemite NPs. Although very high concentrations of hematite NPs (6 g/L) induced very small inhibitory effects on germination and chlorophyll content, all the ferrihydrite treatments showed increased biological indicators. These could be expected because a great variety of agriculturally productive terrains contains naturally occurring ferrihydrite NPs, which may contribute as iron source for plants growth. On the other hand, the translocation of engineered hematite and ferrihydrite NPs into maize stems was shown by 3D microscopic techniques. Clusters of hematite and ferrihydrite NPs were found in endodermis, xylem, phloem vessels, and cell walls of the xylem vessels of maize stems. This study highlights the importance of IO-NPs on germination and seedling growth of maize. However, more studies are necessary, such as the role of both natural and engineered NPs and their effects on other kinds of plants.

Acknowledgements

We would like to thank to Dr. Francisca Ramírez Godina from the Antonio Narro Agrarian Autonomous University, Saltillo, Mexico for the fruitful discussion. We appreciate the assistance of Alvaro Ángeles Pascual for the TEM measurements. NP thanks to Conacyt for the received PhD scholarship. This work was supported by the Multidisciplinary projects initiative of Cinvestav.

References

Alidoust, D., Isoda, A., 2014. Phytotoxicity assessment of gamma-Fe_2O_3 nanoparticles on root elongation and growth of rice plant. Environ. Earth Sci. 71, 5173–5182. http://dx.doi.org/10.1007/s12665-013-2920-z.

Barrena, R., Casals, E., Colón, J., Font, X., Sánchez, A., Puntes, V., 2009. Evaluation of the ecotoxicity of model nanoparticles. Chemosphere 75, 850–857. http://dx.doi.org/10.1016/j.chemosphere.2009.01.078.

Bokare, A.D., Choi, W., 2014. Review of iron-free Fenton-like systems for activating H_2O_2 in advanced oxidation processes. J. Hazard. Mater. 275, 121–135. http://dx.doi.org/10.1016/j.jhazmat.2014.04.054.

Bombin, S., LeFebvre, M., Sherwood, J., Xu, Y., Bao, Y., Ramonell, K., 2015. Developmental and reproductive effects of iron oxide nanoparticles in *Arabidopsis thaliana*. Int. J. Mol. Sci. 16, 24174–24193. http://dx.doi.org/10.3390/ijms161024174.

Briat, J.-F., Curie, C., Gaymard, F., 2007. Iron utilization and metabolism in plants. Curr. Opin. Plant Biol. 10, 276–282. http://dx.doi.org/10.1016/j.pbi.2007.04.003.

Briat, J.-F., Dubos, C., Gaymard, F., 2015. Iron nutrition, biomass production, and plant product quality. Trends Plant Sci. 20, 33–40. http://dx.doi.org/10.1016/j.tplants.2014.07.005.

Briat, J.-F., Duc, C., Ravet, K., Gaymard, F., 2010. Ferritins and iron storage in plants. Biochim. Biophys. Acta 1800, 806–814. http://dx.doi.org/10.1016/j.bbagen.2009.12.003.

Di Bona, K., Xu, Y., Gray, M., Fair, D., Hayles, H., Milad, L., Montes, A., Sherwood, J., Bao, Y., Rasco, J., 2015. Short- and long-term effects of prenatal exposure to iron oxide nanoparticles: influence of surface charge and dose on developmental and reproductive toxicity. Int. J. Mol. Sci. 16, 30251–30268. http://dx.doi.org/10.3390/ijms161226231.

Di Bona, K.R., Xu, Y., Ramirez, P.A., DeLaine, J., Parker, C., Bao, Y., Rasco, J.F., 2014. Surface charge and dosage dependent potential developmental toxicity and biodistribution of iron oxide nanoparticles in pregnant CD-1 mice. Reprod. Toxicol. 50, 36–42. http://dx.doi.org/10.1016/j.reprotox.2014.09.010.

Faraji, M., Yamini, Y., Rezaee, M., 2010. Magnetic nanoparticles: synthesis, stabilization, functionalization, characterization, and applications. J. Iran. Chem. Soc. 7, 1–37.

Giménez, J., Martínez, M., de Pablo, J., Rovira, M., Duro, L., 2007. Arsenic sorption onto natural hematite, magnetite, and goethite. J. Hazard. Mater. 141, 575–580. http://dx.doi.org/10.1016/j.jhazmat.2006.07.020.

González-Melendi, P., Fernández-Pacheco, R., Coronado, M.J., Corredor, E., Testillano, P.S., Risueño, M.C., Marquina, C., Ibarra, M.R., Rubiales, D., Pérez-de-Luque, A., 2008. Nanoparticles as smart treatment-delivery systems in plants: assessment of different techniques of microscopy for their visualization in plant tissues. Ann. Bot. 101, 187–195. http://dx.doi.org/10.1093/aob/mcm283.

Gui, X., Deng, Y., Rui, Y., Gao, B., Luo, W., Chen, S., Van Nhan, L., Li, X., Liu, S., Han, Y., Liu, L., Xing, B., 2015. Response difference of transgenic and conventional rice (*Oryza sativa*) to nanoparticles (γFe_2O_3). Environ. Sci. Pollut. Res. http://dx.doi.org/10.1007/s11356-015-4976-7.

Hong-Xuan, R., Ling, L., Chong, L., Shi-Ying, H., Jin, H., Jun-Li, L., Yu, Z., Xing-Jiu, H., Ning, G., 2011. Physiological investigation of magnetic iron oxide nanoparticles towards Chinese mung bean. J. Biomed. Nanotechnol. 7, 677–684.

Indira, T.K., Lakshmi, P.K., 2010. Magnetic nanoparticles – a review. Int. J. Sci. Nanotechnol. 3, 1035–1042.

Jambor, J.L., Dutrizac, J.E., 1998. Occurrence and constitution of natural and synthetic ferrihydrite, a widespread iron oxyhydroxide. Chem. Rev. 98, 2549–2586. http://dx.doi.org/10.1021/cr970105t.

Li, J., Chang, P.R., Huang, J., Wang, Y., Yuan, H., Ren, H., 2013. Physiological effects of magnetic iron oxide nanoparticles towards watermelon. J. Nanosci. Nanotechnol. 13, 5561–5567. http://dx.doi.org/10.1166/jnn.2013.7533.

Lin, D., Xing, B., 2007. Phytotoxicity of nanoparticles: inhibition of seed germination and root growth. Environ. Pollut. http://dx.doi.org/10.1016/j.envpol.2007.01.016 (Barking, Essex : 1987).

Liu, H., Li, P., Lu, B., Wei, Y., Sun, Y., 2009. Transformation of ferrihydrite in the presence or absence of trace Fe(II): the effect of preparation procedures of ferrihydrite J. Solid State Chem. 182, 1767–1771. http://dx.doi.org/10.1016/j.jssc.2009.03.030.

Lobreaux, S., Briat, J., 1991. Ferritin accumulation and degradation in different organs of pea (*Pisum sativum*) during development. Biochem. J. 274, 601–606.

Lv, J., Zhang, S., Luo, L., Zhang, J., Yang, K., Christie, P., 2015. Accumulation, speciation and uptake pathway of ZnO nanoparticles in maize. Environ. Sci. Nano 2, 68–77. http://dx.doi.org/10.1039/C4EN00064A.

Mahmoudi, M., 2013. Effects of magnetite nanoparticles on soybean chlorophyll. Environ. Sci. Technol. 47, 1645–10652.

Marin, Ş., Lacrimioara, Ş., Cecilia, R., 2011. Evaluation of performance parameters for trace elements analysis in perennial plants using ICP-OES technique. J. Plant Dev. 18, 87–93.

Răcuciu, M., Creangă, D.-E., 2007. Influence of water-based ferrofluid upon chlorophylls in cereals. J. Magn. Magn. Mater. 311, 291–294. http://dx.doi.org/10.1016/j.jmmm.2006.10.1185.

Richmond, W.R., Loan, M., Morton, J., Parkinson, G.M., 2004. Arsenic removal from aqueous solution via ferrihydrite crystallization control. Environ. Sci. Technol. 38, 2368–2372.

Schwertmann, U., Cornell, R.M., 2000. Iron Oxides in Laboratory: Preparation and Characterization, second ed. WILEY-VCH, Weinheim, Germany, doi:10.1097/00010694-199311000-00012.

Siddiqui, M.H., Al-Whaibi, M.H., 2014. Role of nano-SiO_2 in germination of tomato (*Lycopersicum esculentum* seeds Mill.). Saudi J. Biol. Sci. 21, 13–17. http://dx.doi.org/10.1016/j.sjbs.2013.04.005.

Smith, G.S., Johnston, C.M., Cornforth, I.S., 1983. Comparison of nutrient solutions for growth of plants in sand culture. New Phytol. 94, 537–548. http://dx.doi.org/10.1111/j.1469-8137.1983.tb04863.x.

Trujillo-Reyes, J., Majumdar, S., Botez, C.E., Peralta-Videa, J.R., Gardea-Torresdey, J.L., 2014. Exposure studies of core-shell Fe/Fe_3O_4 and Cu/CuO NPs to lettuce (*Lactuca sativa*) plants: are they a potential physiological and nutritional hazard? J. Hazard. Mater. 267, 255–263 http://dx.doi.org/10.1016/j.jhazmat.2013.11.067.

U.S. Environmental Protection Agency, 1996. Ecological Effects Test Guidelines (OPPTS 850.4200): Seed Germination/Root Elongation Toxicity Test.

Wang, Z., Xie, X., Zhao, J., Liu, X., Feng, W., White, J.C., Xing, B., 2012. Xylem- and phloem-based transport of CuO nanoparticles in maize (*Zea mays* L.). Environ. Sci. Technol. 46, 4434–4441. http://dx.doi.org/10.1021/es204212z.

Wu, S.G., Huang, L., Head, J., Chen, D., Kong, I.C., Tang, Y.J., 2012. Phytotoxicity of metal oxide nanoparticles is related to both dissolved metals ions and adsorption of particles on seed surfaces. J. Pet. Environ. Biotechnol. 3, 2–6. http://dx.doi.org/10.4172/2157-7463.1000126.

Xue, X., Hanna, K., Deng, N., 2009. Fenton-like oxidation of Rhodamine B in the presence of two types of iron (II, III) oxide. J. Hazard. Mater. 166, 407–414. http://dx.doi.org/10.1016/j.jhazmat.2008.11.089.

Zhang, T., Liao, X., Yang, R., Xu, C., Zhao, G., 2013. Different effects of iron uptake and release by phytoferritin on starch granules. J. Agric. Food Chem. 61, 8215–8223.

Zhao, L., Peralta-Videa, J.R., Ren, M., Varela-Ramirez, A., Li, C., Hernandez-Viezcas, J.A., Aguilera, R.J., Gardea-Torresdey, J.L., 2012. Transport of Zn in a sandy loam soil treated with ZnO NPs and uptake by corn plants: electron microprobe and confocal microscopy studies. Chem. Eng. J. 184, 1–8. http://dx.doi.org/10.1016/j.cej.2012.01.041.

Zhu, H., Han, J., Xiao, J.Q., Jin, Y., 2008. Uptake, translocation, and accumulation of manufactured iron oxide nanoparticles by pumpkin plants. J. Environ. Monit. 10, 713–717. http://dx.doi.org/10.1039/b805998e.